Reassessing the Structure of Pyranonigrin

Gerhard Schlingmann,*[,†] Tohru Taniguchi,[‡] Haiyin He,[†] Ramunas Bigelis,[†] Hui Y. Yang,[†] Frank E. Koehn,[†] Guy T. Carter,[†] and Nina Berova[‡]

Department of Natural Products, Chemical and Screening Sciences, Wyeth Research, 401 North Middletown Road, Pearl River, New York 10965, and Department of Chemistry, Columbia University, New York, New York 10027

Received April 16, 2007

Fermentation extracts of the marine fungus *Aspergillus niger LL*-LV3020 were found to have relevant activity in a number of assays. Chemical screening of the extracts revealed that this organism produced numerous secondary metabolites in addition to its principal metabolite, citric acid. The compound with the most significant UV peak was isolated and its structure elucidated. Physical data suggested that this compound is identical with pyranonigrin A (**1**); however, our structure elucidation led to a different assignment than previously reported. On the basis of analysis of all data, we propose a correction to the structure of pyranonigrin A. Its absolute configuration was determined by electronic circular dichroism measurements in comparison with theoretical values calculated via *ab initio* time-dependent density functional theory and assigned as (7*R*)-3,7-dihydroxy-2-[(1*E*)-prop-1-enyl]-6,7-dihydropyrano[2,3-*c*]pyrrole-4,5-dione.

In our search for natural products with potential application in human or animal health, we examined methanolic extracts of the marine fungus *Aspergillus niger* (culture *LL*-LV3020) and recognized a number of naphtho-γ-pyrone metabolites[1] with fonsecin[2] as the principal member along with its dehydrated versions rubrofusarin[3] and asperflavone[4] and several dimeric derivatives such as auranosperone B.[4,5] Another group of secondary metabolites was identified as the dicoumarins kotanin,[6] demethylkotanin,[6] and orlandin,[7] which were coproduced with nigragillin,[8] atromentin,[9] and citric acid.[10,11] In fact, the level of citric acid present in the culture extracts was so overwhelming (ca. 35 g/L) that this amount was the root cause of perturbation in the various enzymatic assays. Passing the culture extract through a column with HP20 resin allowed the removal of citric acid from the extract, which could then be further resolved by chromatography on Sephadex LH-20. The collected LH-20 fractions were then thoroughly analyzed by HPLC for known fungal toxins. This procedure led to the isolation of the chief UV-active compound in fractions 9 and 10. Originally we believed that this compound was new, but comparison of our physical data with those published recently for pyranonigrin A[12] revealed that these compounds were identical. However, our interpretation of the data, especially NMR data, did not permit us to assign structure **1a** for pyranonigrin A as reported, but instead led us to conclude that either structure **1c** or **1d** (see Figure 1) was correct. To resolve this matter, we undertook an extensive analysis of the compound and corroborated its structure assignment as **1d**. Here, we wish to report the results of our investigation including a re-examination of the absolute configuration of pyranonigrin A.

Results and Discussion

Isolation. Pyranonigrin A (**1**), seen as the major UV peak in the chromatogram shown in Figure 2, was readily isolated from solid fermentations of culture *LL*-LV3020 by extracting the solids with MeOH followed by resin adsorption on HP20 and chromatography on Sephadex LH-20. Fraction 9 of the Sephadex LH-20 chromatography yielded nearly white, solid material of pyranonigrin A (**1**) that contained a small amount of its congener pyranonigrin S (**2**). Repeated attempts to obtain crystalline material by slow evaporation of the solvent were unsuccessful and apparently resulted in some decomposition, as judged by darkening (browning) of the solution. Most spectroscopic analyses were performed on the reprecipitated material obtained in fraction 9.

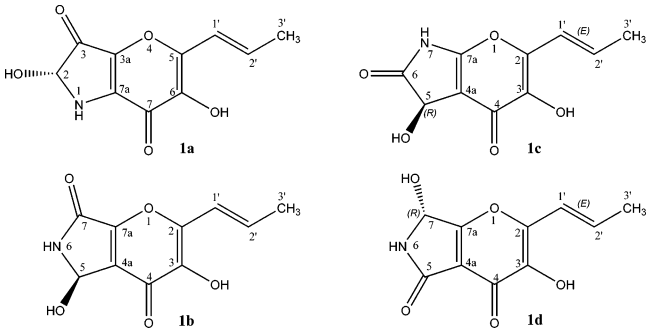

Figure 1. Structural isomers considered for the representation of pyranonigrin A (note the different numbering system for structure **1a**).

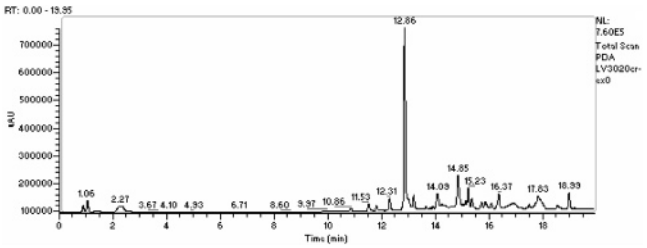

Figure 2. HPLC profile of a crude methanolic extract of culture *LL*-LV3020.

Structure Elucidation. Similar to the previous report,[12] our structure determination of the pyranonigrin components is based on the interpretation of spectrometric and spectroscopic data, especially MS and NMR data, which include COSY, ROESY, HSQC, HMBC, and an essential $^{1}H-^{15}N$ HMBC. On the basis of heteronuclear NMR correlations, the core structure of **1** was readily recognized as a γ-pyrone unit substituted with a propenyl side chain, as shown in Figure 1 or 3, which is in agreement with published observations.[12] However, the assignment of the molecule as either 3,5-dihydroxy-2-(prop-1-enyl)pyrano[2,3-*b*]pyrrole-4,6(5*H*,7*H*)-dione (**1c**) or 3,7-dihydroxy-2-(prop-1-enyl)-6,7-dihydropyrano[3,2-*c*]pyrrole-4,5-dione (**1d**) was a difficult feat and could not be accomplished unambiguously without taking into account the reactivity of its diacetate derivative described below.

To assign the correct structure of **1**, containing a lactam ring, we have to consider four eligible isomers (**1a**−**1d**, shown in Figure

* To whom correspondence should be addressed. Tel: (845) 602-4390. E-mail: schling@wyeth.com.
† Wyeth Research.
‡ Columbia University.

10.1021/np070175n CCC: $37.00
Published on Web 06/30/2007

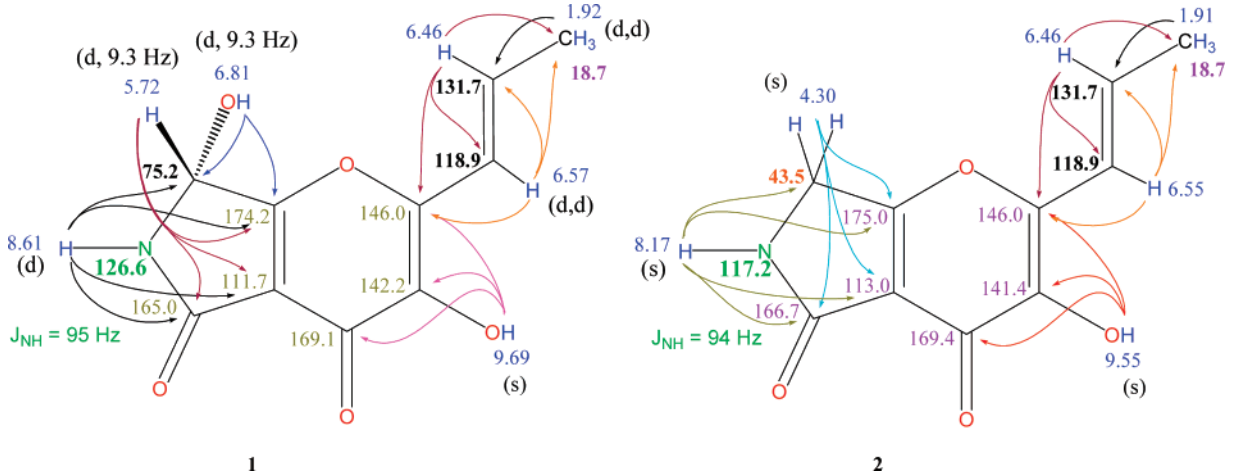

Figure 3. Structures of pyranonigrin A (**1**) and pyranonigrin S (**2**) with NMR chemical shift assignments and observed HMBCs (arrows) recorded in DMSO-d_6 solutions.

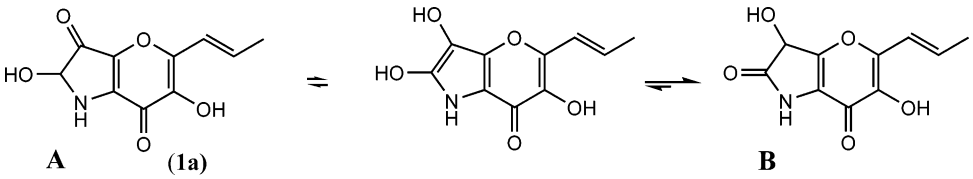

Figure 4. Energy calculations on tautomers of structure **1a** favor structure **B** as the most stable form.

1). Of these, structure **1a**, previously published as pyranonigrin A,[12] can clearly be dropped from further consideration on the basis of the following observation. A $^1H-^{15}N$ HMBC NMR experiment showed the ^{15}N chemical shift for the nitrogen atoms in both **1** and **2** to be at 126.6 and 117.2 ppm, respectively. This chemical shift is consistent only with an amide nitrogen but not with the hemiaminal function of structure **1a**, where the ^{15}N atom is expected to resonate near (δ_N) 80 ppm. Further, the ^{13}C chemical shift of the 3-keto group, precedented with 197.0 ppm for matemone,[13] is predicted to be near 190 ppm for **1a**, which is in contrast to the reported shift of 174 ppm. Last, analogous to observations made on certain N-heteroaromatic compounds[14] and dioxindole,[15] the postulated structure **1a** (**A** in Figure 4) is expected to be the minor form of several possible keto−enol tautomers of which the 2-oxo form (**B**) would be the prominent species. Although structures **A** and **B** were discussed in the previous publication[12] as to their compliance with observed ROESY signals, apparently little attention was paid to their probable existence.

The predicted ^{13}C chemical shift values for C-4a and C-7a of structure **1b**, as well as the equivalent carbon atoms C-3a and C-7a for the 2-oxo tautomer of structure **1a** (**B** in Figure 4), range from 130 to 134 ppm in the case of C-4a (C-7a) and from 149 to 158 ppm in the case of C-7a (C-3a). Therefore, these structures can be excluded from further consideration, as the predicted chemical shift values are out of range with respect to the observed ^{13}C chemical shifts of 112 (C-4a) and either 165 or 174 ppm (C-7a), respectively. Besides the one required amide resonance, a second, low-field chemical shift is expected only when the 4a−7a carbon bridge is polarized by the electron-withdrawing effect of either two heteroatoms bonded to the same carbon atom (as is the case for structure **1c**) or two augmenting, conjugated keto(carboxyl or amide) groups, as is the case for structure **1d**, but not structure **1b**. Therefore, both structures (**1c** and **1d**) would fit the NMR chemical shift data for pyranonigrin A and are also fully supported by predicted ^{13}C chemical shift values.

Although structure **1d** seemed to provide the better match for the data, the small magnitude of the coupling constant between H-6 and H-7 (J < 1.0 Hz) provided an uncertainty whether it was due to a vicinal (in the case of structure **1d**) or a homoallylic coupling (in the case of structure **1c** between H-5 and H-7). These

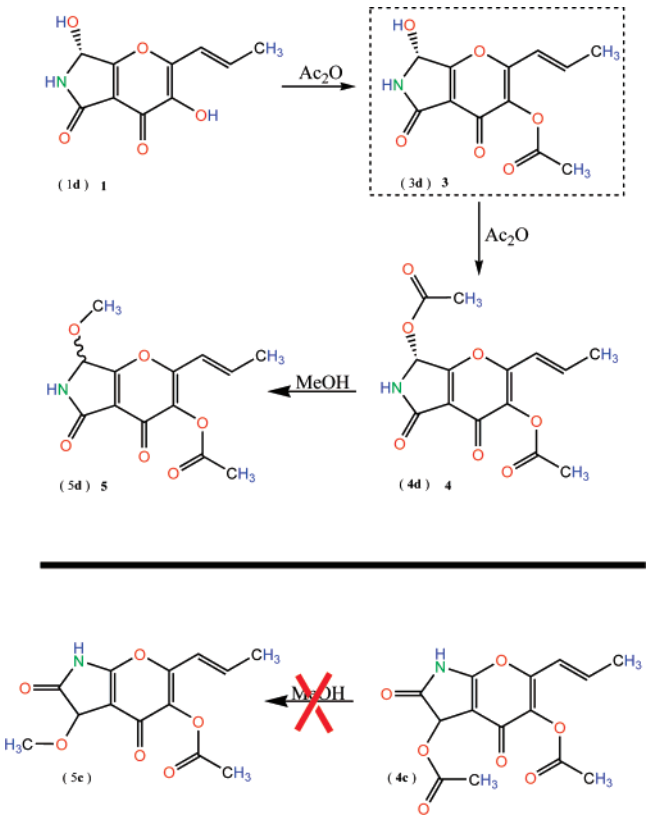

Figure 5. Replacement of the acetate group in **4** by MeOH can only occur in structure **4d**.

protons also correlated in the ROESY spectrum, which would be difficult to explain for structure **1c** unless the pyrrolone ring would buckle severely, an unlikely occurrence.

On the other hand, our initial preference for structure **1c** was derived from reports on a number of natural products containing a reduced maleimide moiety, such as integramycin,[16] the delaminomycins,[17] quinolactacin C,[18] and jatropham,[19] that indicated a facile

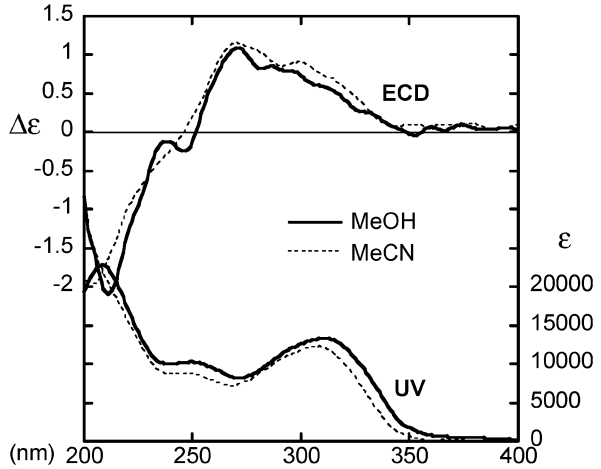

Figure 6. ECD and UV spectra of pyranonigrin A (**1**) measured in MeOH (c = 0.25 M, solid line) and in MeCN (c = 0.05 M, dotted line).

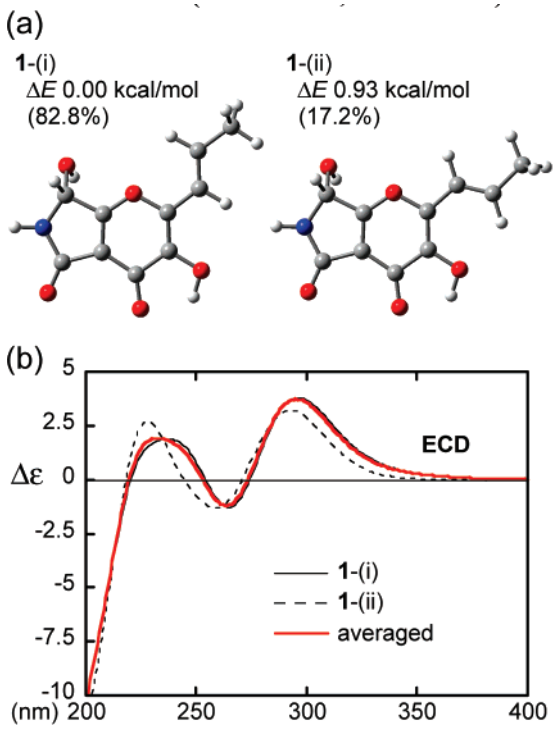

Figure 7. (a) Stable conformers of (*R*)-**1** optimized at the DFT/B3LYP/6-31G(d) level, along with the free energy differences and the Boltzmann populations. (b) Theoretical ECD spectra for each conformer and their population-weighted average calculated at the TDDFT/B3LYP/aug-cc-pVDZ level.

racemization at its stereogenic center involving the 5-hydroxy group and/or reaction of the 5-hydroxy group itself. In fact, dissolving 5-hydroxy-4-methoxy-1*H*-pyrrol-2(5*H*)-one in MeOH/HCl converted the compound quantitatively to 4,5-dimethoxy-1*H*-pyrrol-2(5*H*)-one.[20] In contrast, pyranonigrin A (**1**) could be kept in methanolic solution (original extract) without forming a methylated derivative. Acidic catalysis of this reaction could potentially have occurred by the copious amount of citric acid present. However, controlled CD measurements on **1** kept in MeOH showed no decrease in optical activity over time. We also studied the H−D exchange rate of the H-7 hydrogen atom [δ_H 5.79] (H-5 in structure **1c**) at ambient temperature by keeping **1** in the deuteriated NMR solvent, MeOH-d_4, and found that there was no exchange over the 8-week study period; integration data of the methyl resonance (position 3′) were used as internal reference.

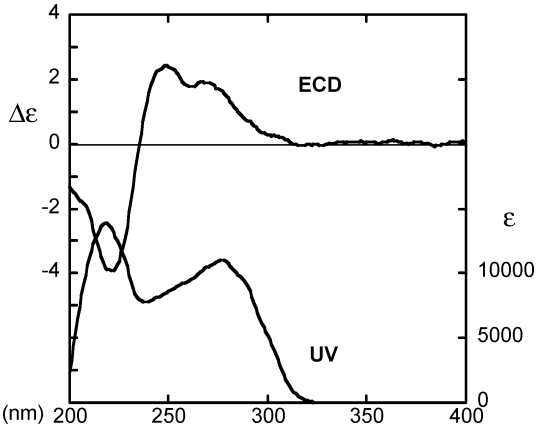

Figure 8. ECD and UV spectrum of 3,7-di-*O*-acetylpyranonigrin A (**4**) measured in MeCN (c = 0.25 M).

Unambiguous evidence in favor of structure **1d** was eventually derived from the reactivity of its diacetate derivative **4**, which readily converted to **5** in methanolic solution. Addition of $NaHCO_3$ accelerated this reaction significantly. The initial purpose of preparing the monoacetate derivative **3** and the diacetate **4**, as well as the 3-ethoxy derivative **6**, was to obtain hydrophobic derivatives suitable for comparison of experimental UV/CD spectra with that of *ab initio* predicted data (*in vacuo*), since **1** itself is soluble only in polar solvents.

Treating **1** with Ac_2O at 65 °C overnight yielded di-*O*-acetylpyranonigrin A (**4**). Initially, this reaction was conducted at ambient temperature, but under these conditions the conversion was still incomplete after 5 days. Since the 3-OH group is part of the chromophore, derivatization at this position impacts the chromophore, and therefore, the two monoacetate derivatives (at position 3 versus position 7) were readily distinguished by their respective UV spectra. We followed the progress of the acetylation reaction by LC-MS analysis and established that **1** preferentially reacts at its 3-OH position, which is indicated by the hypsochromic shift of the maximum in its UV spectrum from 314 to 286 nm, while the UV spectrum of the monoacetate attached at C-7 is virtually indistinguishable from that of **1**. Due to the 3-*O*-acetyl group, monoacetate **3** and the diacetate **4** have the same chromophore and thus nearly identical UV spectra. It should be noted that at no time during the acetylation reaction was there an indication that the NH function could be acetylated, bolstering evidence that the NH function was part of a nonreactive lactam ring. If structure **1a** had been correct, then the acetylation would have provided a triacetate derivative.

Most data on diacetate **4** were recorded on the crude reaction residue (see Experimental Section), as purification and maintenance of **4** in pure form proved difficult due to the reactivity of its 7-acetate group. This reactivity was first noticed after a failed purification attempt by reversed-phase chromatography using standard conditions (MeCN/H_2O/0.01 M TFA). Although the chromatography was uneventful, as anticipated from the analytical LC-MS results (Figure 9), concentration (SpeedVac) of the fraction containing diacetate **4** yielded a dark, gluey mass that could not be further characterized. Therefore, a second purification was attempted to separate **4** from dark brown, nonspecific impurities under the milder conditions of LH20 chromatography. Unexpectedly, after a 1 h run time the column effluent contained two components, starting material **4** and its methanolysis product **5**, in a 1:1 ratio. Compound **5** was identified by its molecular ion ([M + H]$^+$ = m/z 280.1) in the LC-MS and by NMR as a mixture and after purification. The HMBC spectrum of **5** revealed cross-peaks from the methoxy group [δ_H 3.38] to C-7 [δ_C 81.7] and from H-7 [δ_H 5.70] to the methoxy group [δ_C 54.3], carbamide C-5 [δ_C 166. 1], and C-7a [δ_C 172. 7] and weakly to C-4a [δ_C 115. 2]. Further correlations from the NH

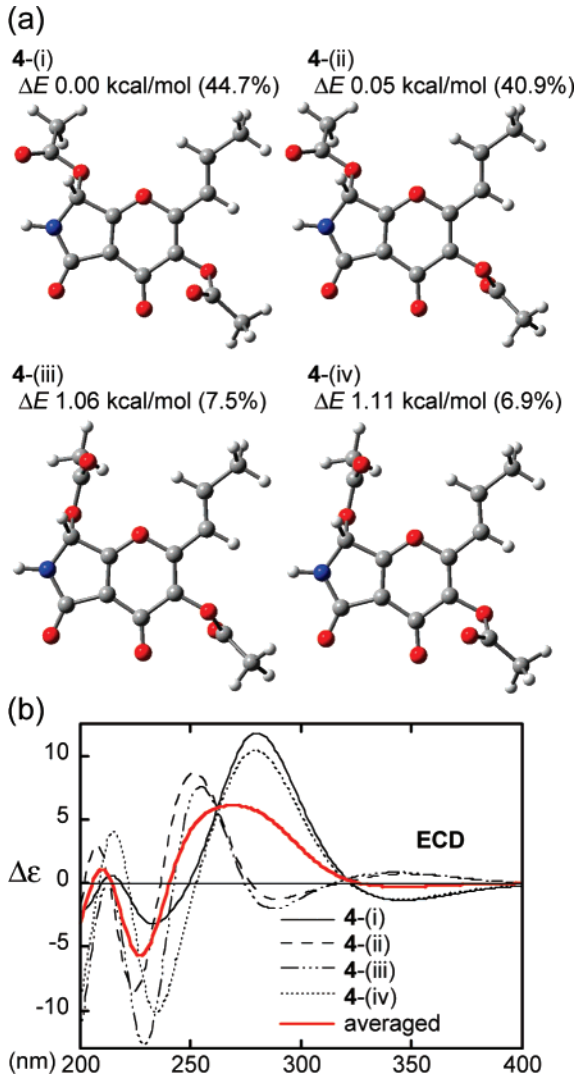

Figure 9. (a) Stable conformers of (*R*)-**4** optimized at the DFT/B3LYP/6-31G(d) level, along with the free energy differences and the Boltzmann populations. (b) Theoretical ECD spectra for each conformer and their population-weighted average calculated at the TDDFT/B3LYP/aug-cc-pVDZ level.

proton [δ_H 8.06] to the methine carbon C-7 [δ_C 81.7], C-4a [δ_C 115. 2], and C-7a [δ_C 172. 7] and weakly to carbamide C-5 [δ_C 166. 1] supported the conclusion that the methoxy group of **5** had replaced the 7-hydroxy group of **1** by substituting the 7-acetate group of **4**.

As Figure 5 illustrates, this substitution reaction is feasible only when **1** is assigned structure **1d** and not **1c**, because only in the acetylated version (**4d**) can the acetate moiety be substituted directly by a methoxy group; there is ample precedence for this reaction.[21−23]

Although pyranonigrin S (**2**) was co-purified with pyranonigrin A (**1**) as a minor co-metabolite, isolation of pyranonigrin S (**2**) as a single compound was not attempted. Nevertheless, given the structure of **1**, the availability of physical data from in-line processes such as LC-UV-MS and the great similarity between the UV spectra of **1** and **2**, the structure of **2** was readily elucidated from NMR data obtained on the pyranonigrin mixture containing ca. 10% of **2**. As the molecular mass of **2** was 16 Da less than that of **1** and its corresponding NMR data lacked the resonance for the single 7-H (and 7-OH) group, and instead revealed a CH_2 resonance [δ_C 43.5] that showed a negative cross-peak to a singlet at δ_H 4.30 in the phase-sensitive HSQC spectrum along with other relevant homo- and heteronuclear correlations connecting it to the pyrone ring and the amide group, the structure of **2** was elucidated as revealed in Figure 3.

Absolute Configuration. The absolute configuration of compound **1** as (7*R*)-3,7-dihydroxy-2-[(1*E*)-prop-1-enyl]-6,7-dihydropyrano[2,3-*c*]pyrrole-4,5-dione was determined by a nonempirical analysis of electronic circular dichroism (ECD) using a recently developed, time-dependent density functional theory (TDDFT) calculation method.[24−27] The UV and ECD spectra of **1**, measured in MeOH as well as MeCN, are presented in Figure 6. The ECD spectrum of the MeOH solution featuring a broad positive band in the range 250−350 nm with a maximum at around 270 nm and a negative mimimum at around 210 nm agreed well with the one previously reported.[12]

It has been suggested that hydrocarbons, such as hexane, are the best solvents for comparison between experimental and calculated properties of an isolated molecule.[28] More recently, however, other studies have shown that solvents possessing high dielectric constants, such as MeCN, permit a better comparison between experimental chiroptical data and theoretical data as calculated for the isolated molecule.[29] Since **1** was insoluble in hydrocarbons and ethers, but soluble in MeCN and MeOH, its ECD spectra were measured in these two solvents. The spectrum in MeCN exhibited peak patterns quite similar to those observed in MeOH with only minor differences, as indicated in Figure 6, implying that the positive−negative band pattern of **1** is independent of solvent effects.

Prior to the calculation of chiroptical properties, a conformational analysis was carried out to define stable conformations and their relative energies. Arbitrarily starting with the *R* absolute configuration, an initial conformational distribution survey was performed using a Monte Carlo search together with the MMFF94 molecular mechanics force field. The resulting stable conformers were then optimized using density functional theory (DFT) at the B3LYP/6-31G(d) level in vacuum conditions, leading to two stable conformations, **1**-(i) and **1**-(ii), that differed in the rotation around the C2−C1′ bond (Figure 7a). Further, it was found that the 3-hydroxy group was preferably oriented toward the neighboring 4-keto group, where the distance between the 3-hydroxy hydrogen atom and the oxygen atom of the 4-ketone was estimated to be ca. 2.0 Å, thus implying a stabilizing effect from intramolecular hydrogen bonding. To minimize the steric hindrance, the hydrogen atoms at C-7 and the 7-OH function assume preferentially the *anti* conformation, which is also evident from their large coupling constant ($^3J_{H,OH}$ = 9.3 Hz) in the ^{1}H NMR spectrum.

The ECD spectrum of each conformer of (*R*)-**1** was calculated at the TDDFT/B3LYP/aug-cc-pVDZ level considering the 40 lowest energy transitions. The theoretical spectrum was finally obtained as a weighted average based on their Boltzmann populations (Figure 7b, red line) and compared with the experimental ECD spectrum. Both experimental and predicted spectra showed a broad positive band in the longer wavelength region and a negative band in the shorter wavelength region, suggesting that the absolute configuration is *R*. However, an incongruity was recognized in the region around 235 nm, where the calculated ECD spectrum exhibited a positive band, while the experimental spectra showed this feature only as a subtle band. It is well-known that alcohols tend to hydrogen-bond intermolecularly with solvent or solute molecules,[30] which alters the conformational population and the electronic state of the analyzed molecule, giving it a different environment than that simulated for the isolated state. Several recent publications reported derivatization of the analyte to avoid solvent effects and/or intermolecular aggregation.[31−33] Therefore, the ECD spectrum of diacetate **4** was included in our analysis in order to minimize any solvation effect that could possibly account for erroneous results.

The experimental UV and ECD spectra of **4** measured in MeCN are shown in Figure 8. Similar to that observed for **1**, the ECD spectrum shows a broad positive band in the longer wavelength region (with two maxima at 266 and 249 nm) and a negative band in the shorter wavelength region (at around 220 nm). Conforma-

tional and ECD calculations for (*R*)-**4** employed a similar protocol to that applied to the calculations for the (*R*)-**1** configuration. The conformational search and the follow-up optimization identified four conformers that were within 2 kcal/mol of the most stable form. This search revealed that any conformational flexibility is derived from the potential rotation around the ester bond of each acetate group, while the propenyl unit preferred the *s-trans* conformation to avoid steric hindrance with the 6-acetate group (Figure 9a). The ECD spectra for these conformations were calculated and averaged according to their Boltzmann population and then compared with the experimental spectrum (Figure 9b). All of the predicted spectra for the individual conformers showed a positive band at around 250 to 275 nm and a negative band at around 230 nm. As a result, the weighted spectra accurately reproduced the observed positive and negative features of the experimental ECD spectrum and thus verified the *R*-assignment for **4** as previously concluded for underivatized **1**.

Conclusion

The main UV-active compound produced in fermentations with *A. niger LL*-LV3020 was found to be identical with a reported *A. niger* metabolite named pyranonigrin A (**1a**)[12] by comparison of available physical data. However, our analysis of the data arrived at a different structure than that previously assigned. On the basis of a follow-up evaluation of all data, including the observed reactivity of the diacetate derivative, we now propose a correction to the structure of pyranonigrin A as disclosed herein with structure **1d** (Figure 1) or **1** (shown in Figure 3) as (7*R*)-3,7-dihydroxy-2-[(1*E*)-prop-1-enyl]-6,7-dihydropyrano[2,3-*c*]pyrrole-4,5-dione having the *R*-absolute configuration at C-7.

Comparing the structure of **1** with known natural products reveals that the fungal metabolites phaeosphaeride A,[34] curvupallides,[35] and rubrobramide[36] are its closest relatives since they incorporate the same core skeleton. It could be argued that the pyranonigrins are also related to the himeic acids[37] or microsphaerones[38] as well, since these have a γ-pyrone unit in common. The massarilactones,[39] metabolites from an aquatic fungus with similar structures, may also belong to this group.

Although the production of pyranonigrin A appears to be associated with *A. niger* strains isolated from marine sources, other aspergilli also produce this metabolite. In fact, we first detected pyranonigrin A in a fermentation extract derived from a terrestrial fungus, *A. niger LL*-RB17, which was isolated from a banana of Ecuadoran origin. A recent analysis of extrolites[40] from a number of aspergilli, many of which were isolated from terrestrial sources, confirms that the production of pyranonigrin A is not limited to fungi from marine environments.

Experimental Section

General Experimental Procedures. Optical rotation at the sodium-D line was measured using a JASCO DIP-1000 digital polarimeter. UV and ECD spectra were measured on a JASCO V-530 spectrophotometer and a JASCO J-810 spectropolarimeter, respectively, and presented in molar absorptivity, ϵ (L/mol·cm). UV spectra were also obtained on peaks during chromatographic separations with diode array detectors (see chromatographic equipment).

An Agilent 1100 LC system equipped with a Phenomenex Prodigy ODS-3 (4.6 × 250 mm, 5 μm) HPLC column using a linear gradient of 45 to 90% MeOH with and without the addition of TFA, at a flow rate of 1.0 mL/min, was used to chromatographically separate the metabolites produced by culture *LL*-LV3020 (see Figure 2). The composition of the eluting solvent was preprogrammed as a mixture of three solvents (solvent A: 100% double distilled H_2O; solvent B: 100% MeOH, solvent C: 0.2% aqueous TFA) to result in the indicated gradient: 35% A to 90% B over 20 min, while C was metered at a constant rate of 10%; the final mixture of 90% B and 10% C was held for 10 min and then returned to starting conditions. A YMC ODS-A (4.6 × 250 mm, 5 μm) C_{18} HPLC column eluted with a linear gradient from 50 to 90% was also used to achieve similar results.

LC-MS data were obtained on a Thermoquest LCQ Deca instrument equipped with an Agilent 1100 LC system including a diode array detector and a YMC ODS-A column (0.2 × 10 cm, 3 μm); flow 0.3 mL/min (solvent A: 0.025% formic acid in H_2O; solvent B: 0.025% formic acid in MeCN; gradient: 5% B to 95% B into A over 20 min, then holding for 10 min). A total scan UV chromatogram is acquired over a scan range from 190 to 500 nm. UV spectra are acquired on the fly over the same range with scan steps of 2 nm. After emerging from the UV flow cell, the effluent stream goes into the ion trap mass spectrometer. The mass spectrometer is fitted with an electrospray ionization (ESI) probe and is operated in alternating positive-ion and negative-ion full scan (100−2000 mass units) mode. The spray needle voltage is set to 6 kV for positive and 4.5 kV for negative. The capillary voltages are set at 29 and −10 for positive and negative ion detection, respectively. The capillary temperature is set to 200 °C. Nitrogen is used as the sheath and auxiliary gases, which are set to 60 and 25 units, respectively.

A preparative purification of LV3020 metabolites was achieved by using a larger YMC ODS-A column (1 × 25 cm, 5 μm) and a flow rate of 4 mL/min instead of 1 mL/min, under otherwise identical conditions as outlined above.

NMR spectra were recorded on a Bruker Avance DPX-400 or 500 MHz NMR spectrometer at 400 (500) and 100 (125) MHz for ^{1}H and ^{13}C, respectively, using a 3 mm broad-band probe. Chemical shifts are given in ppm relative to the solvent signals of DMSO-d_6 (δ_H 2.49, δ_C 39.50), acetone-d_6 (δ_H 2.04, δ_C 29.81), $CDCl_3$ (δ_H 7.26, δ_C 77.00), or MeOH-d_3 (MeOH-d_4) (δ_H 3.30, δ_C 49.00), respectively. ^{15}N chemical shifts were measured indirectly, via ^{1}H−^{15}N long-range correlation by means of the J_{H-N}-HMBC experiment of samples in DMSO-d_6 solution, with the following parameters: relaxation delay 100 ms, scaling factor 23, J = 4 Hz, 180 scans. For this experiment the instrument was calibrated to the external ^{15}N reference shift for liquid ammonia (δ_N = 0 ppm).

All solvents were obtained from J. T. Baker, Inc. and were of the highest commercially available purity.

Computational Method. The preliminary conformational distribution search was performed by a Spartan02 program using the MMFF94s molecular mechanics force field. The lower energy conformers that differ from the most stable one by less than 10 kcal/mol were further fully optimized at the DFT/B3LYP/6-31G(d) level as implemented in Gaussian03 software. Several conformers within 2 kcal/mol from the most stable one have been taken into account for ECD calculations, following a generally accepted protocol.

All the ECD computations were carried out by means of Gaussian03 software employing the TDDFT approach, the B3LYP functional, and the aug-cc-pVDZ basis set. The first 25 or 40 singlet → singlet electronic transitions were considered. The calculated ECD spectra in $\Delta\epsilon$ units have been obtained by using Gaussian band shapes and 0.18 eV half-width at 1/e of peak height.

Isolation and Purification of Pyranonigrin. A seed culture of *A. niger LL*-LV3020, a marine fungus isolated from mangrove wood in the coastal environment of Hong Kong, was first grown on Difco potato-dextrose broth for 4 days. This 50 mL seed medium was agitated in a 250 mL Erlenmeyer flask at 200 rpm, at 22 °C, and then used to inoculate larger flasks bearing solid medium for production of desired metabolites. A volume of 17.5 mL of seed medium was used to inoculate a 2.8 L Fernbach flask containing a sterile mixture of 72 g of corn, 90 g of rice, and 18 g of blended alfalfa moistened with 88 mL of 0.1% Difco yeast extract. The production flasks were incubated under stationary conditions at 22 °C, and fungal mycelia showed prolific growth on the solid substrate upon harvest after 2 weeks. A 2.8 L production culture was harvested by adding MeOH (1000 mL) and mechanically stirring the mash for approximately 1 min. This methanolic mixture was kept for 1 day at room temperature, then filtered, and the solids were washed with additional MeOH. The combined methanolic extracts were concentrated to approximately 120 mL of a viscous, black mixture containing approximately 41 g of solid material, most of which was citric acid.

This crude, blackish-green extract was slurried with 200 mL of CH_2Cl_2, causing the precipitation of a black paste on the bottom of the flask. Following decanting, the settled black paste was triturated with 200 mL of EtOAc for 1 h, and the solution was then decanted and concentrated, yielding 2.64 g of solids that were set aside for further processing. The remaining solids were dissolved in 250 mL of H_2O and passed over a prepared HP20 column (2.5 × 12 cm) and washed

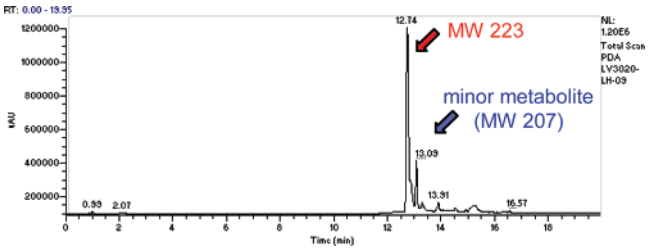

Figure 10. HPLC trace of isolated pyranonigrins A and S.

with 50 mL of H_2O. Effluent and wash, essentially containing only citric acid, were discarded, and the HP20 columm was then eluted with MeOH. This MeOH extract yielded 1.40 g of solids, which was charged as a concentrated, methanolic solution onto a prepared Sephadex LH-20 column (2.5 × 42 cm) and developed with MeOH. Fractions of 40 mL each were collected at regular intervals and analyzed by LC-MS for content as described above. The fractions were dried by centrifugal evaporation (SpeedVac), yielding pyranonigrin in fractions 8 to 11 as yellowish solids. The solid material (152.8 mg) of the peak tube in fraction 9 was triturated several times with acetone, and the resulting acetone solutions were dried under a stream of N_2, depositing an off-white solid (64 mg) in the collecting glass vial. The HPLC trace of the solids thus obtained is shown in Figure 10.

Physicochemical Properties of Pyranonigrins. 1 (Pyranonigrin A), (7*R*)-3,7-dihydroxy-2-[(1*E*)-prop-1-enyl]-6,7-dihydropyrano[2,3-*c*]pyrrole-4,5-dione: $C_{10}H_9NO_5$ MW 223.18 (see Figure 3); $[\alpha]_D^{25}$ +42.4 ± 1 (*c* 1.15%, MeOH); $[\alpha]_D^{25}$ +38.2 (*c* 1.0 mg/dL, MeOH); $[\alpha]_D^{25}$ +84.4 (*c* 1.0 mg/dL, DMSO); UV (MeOH) λ_{max} nm (ϵ) 210 (19 400), 250 (9900), 314 (13 200); UV (MeCN/H_2O) λ_{max} nm (ϵ) 208, 250, 312; IR (KBr) 3288, 2981, 2671, 1716(s), 1654(s), 1636(s), 1615, 1395, 1219, 1035 cm^{-1}; ^1H NMR (DMSO-d_6, see Figure 3) δ_H 9.69(s, 1H, [3-O*H*]), 8.61(d, $^3J_{H,H}$ = 0.8 Hz, J_{NH} = 95 Hz, 1H, N*H*), 6.81(d, 1H, [7-O*H*], $^3J_{H,H}$ = 9.3 Hz), 6.57(dd, 1H, [H-1′], $^3J_{H,H}$ = 15.9 Hz), $^4J_{H,H}$ = 1.7 Hz, $J_{C,H}$ = 160.5 Hz), 6.46(dq, 1H, [H-2′], $^3J_{H,H}$ = 15.9 Hz, $^3J_{H,H}$ = 6.7 Hz, $J_{C,H}$ = 159.7 Hz), 5.72(dd, 1H, [H-7], $^3J_{H,H}$ = 9.3, 0.8 Hz, $J_{C,H}$ = 163.2 Hz), 1.92(dd, 3H, [3′-C*H*$_3$], $^3J_{H,H}$ = 6.7 Hz, $^4J_{H,H}$ = 1.7 Hz, $J_{C,H}$ = 127.8 Hz); ^{13}C NMR (DMSO-d_6, see Figure 3); ^1H NMR (acetone-d_6) (see Table 1); ^{13}C NMR (acetone-d_6) (see Table 1); ^1H NMR (MeOH-d_3) δ_H 6.63(2H, m), 5.79(1H, s), 1.96(3H, d); ^{13}C NMR (MeOH-d_3) δ_C 175.5(s), 171.0(s), 167.1(s), 148.6(s), 143.6(s), 133.7(d), 119.9(d), 112.8(s), 77.2(d), 19.0(q); MS (ESI-pos) $[M + H]^+$ = *m/z* 224.1 (100%); $[M + NH_4]^+$ = *m/z* 241.0 (30%); $[2M + H]^+$ = *m/z* 247.0 (45%); MS (ESI-neg) $[M - H]^-$ = *m/z* 222.0 (4%), $[M + HCOO]^-$ = *m/z* 267.1 (3%).

2 (Pyranonigrin S), 3-hydroxy-2-[(1*E*)-prop-1-enyl)]-6,7-dihydropyrano[2,3-*c*]pyrrole-4,5-dione): $C_{10}H_9NO_4$ MW 207.18 (see Figure 3); UV (MeCN/H_2O) λ_{max} nm (ϵ) 210 (18 000), 250 (8100), 312 (13 300); ^1H NMR (DMSO-d_6, see Figure 3) δ_H 9.55(s, 1H, [3-O*H*]), 8.17(s, J_{NH} = 94 Hz, 1H, N*H*), 6.55(dd, 1H, [H-1′], $^3J_{H,H}$ = 15.9 Hz), $^4J_{H,H}$ = 1.7 Hz), 6.46(dq, 1H, [H-2′], $^3J_{H,H}$ = 15.9 Hz, $^3J_{H,H}$ = 6.7 Hz), 4.30(s, 2H, [H-7], $J_{C,H}$ = 145.1 Hz), 1.91(dd, 3H, [3′-C*H*$_3$], $^3J_{H,H}$ = 6.7 Hz, $^4J_{H,H}$ = 1.7 Hz); ^{13}C NMR (DMSO-d_6, see Figure 3); MS (ESI-pos) $[M + H]^+$ = *m/z* 208.1 (100%), $[M + NH_4]^+$ = *m/z* 225.0 (40%); MS (ESI-neg) $[M - H]^-$ = *m/z* 206.0 (2.8%).

Acetylation of Pyranonigrin. Ac_2O (10 mL) was added to pyranonigrin A (4.8 mg, 0.022 mmol), and the mixture stirred at room temperature. The reaction was monitored by TLC. After 7 days, the solvent was evaporated and the residue was subjected to silica gel column chromatography ($CHCl_3$/MeOH, 19:1), affording 0.6 mg of di-*O*-acetylpyranonigrin A: HRMS (FAB) *mlz* for $C_{14}H_{14}NO_7$ ($[M + H]^+$), calcd 308.0770, found 308.0784.

Dry, (white) powdery material of **1** (30 mg) was dissolved in 10 mL of Ac_2O (in a 20 mL vial with screw top), gently heated to 65 °C, and kept at that temperature overnight, during which time the yellow solution turned brown. The reaction was monitored by LC-MS analysis using the Thermoquest LCQ Deca instrument described above. The chromatogams (Figure 11) show a four-component mixture 6 h into the acetylation reaction, whereas the bottom panel shows the final product after overnight reaction and solvent removal. The solvent (HOAc and Ac_2O) was removed under a stream of N_2 until solid, glass-like material remained. This procedure was repeated twice by adding acetone to allow residual HOAc to evaporate. The remaining solid (46 mg) was used directly for NMR experiments.

3 (3-*O*-Acetylpyranonigrin A), (7*R*)-7-hydroxy-4,5-dioxo-2-[(1*E*)-prop-1-enyl)]-4,5,6,7-dihydropyrano[2,3-*c*]pyrrole-3-yl acetate: $C_{12}H_{11}NO_6$ MW 265.22 (see Figure 5); UV (MeCN/H_2O) λ_{max} nm 216, 250 (sh), 286; ^1H NMR (acetone-d_6) (see Table 1); ^{13}C NMR (acetone-d_6) (see Table 1); MS (ESI-pos) $[M + H]^+$ = *m/z* 266.2 (50%), $[M + NH_4]^+$ = *m/z* 282.9 (60%), $[2M + NH_4]^+$ = *m/z* 547.9 (100%); MS (ESI-neg) $[2M + HCOO]^-$ = *m/z* 575.0 (2.8%).

4 (3,7-Di-*O*-acetylpyranonigrin A), (7*R*)-4,5-dioxo-2-[(1*E*)-prop-1-enyl)]-4,5,6,7-tetrahydropyrano[2,3-*c*]pyrrole-3,7-diyl diacetate: $C_{14}H_{13}NO_7$ MW 307.26 (see Figure 5); UV (MeCN/H_2O) λ_{max} nm (ϵ) 218, 250 (sh), 284; ^1H NMR ($CDCl_3$) δ_H 7.85(br s, 1H, N*H*), 6.76(m, 1H, [H-2′], $^3J_{trans}$ = 15.8 Hz, $^3J_{H,H}$ = 7.0 Hz), 6.29(dd, 1H, [H-1′], $^3J_{trans}$ = 15.8 Hz, $^4J_{H,H}$ = 1.5 Hz), 6.65(d, 1H, [H-7], $^3J_{H,H}$ = 1.5 Hz), 2.32(s, 3H, [3-OCOC*H*$_3$]), 2.14(s, 3H, [7-OCOC*H*$_3$]), 1.96(d, 3H, [3′-C*H*$_3$], $^3J_{H,H}$ = 7.0 Hz, $^3J_{H,H}$ = 1.5 Hz); ^{13}C NMR ($CDCl_3$) δ_C 171.5(s, C-7a), 170.1(s, O*C*OCH$_3$), 167.4(s, O*C*OCH$_3$), 167.0(s, C-4), 165.4(s, C-5), 155.2(s, C-2), 138.6(d, C-2′), 136.5(s, C-3), 117.0(d, C-1′), 115.2-(s, C-4a), 75.0(d, C-7), 20.5(q, 7-OCO*C*H$_3$), 20.1(q, 3-OCO*C*H$_3$), 18.9-(q,C-3′); ^1H NMR (acetone-d_6) (see Table 1); ^{13}C NMR (acetone-d_6) (see Table 1); ^1H NMR (acetone-d_6) δ_H 8.04(br s, 1H, N*H*), 6.86(d, 1H, [H-7], $^3J_{H,H}$ = 0.8 Hz, $J_{C,H}$ = 172.0 Hz), 6.80(d,q, 1H, [H-2′], $^3J_{trans}$ = 15.8 Hz, $^3J_{H,H}$ = 7.0 Hz, $J_{C,H}$ = 166.0 Hz), 6.54(dd, 1H, [H-1′], $^3J_{trans}$ = 15.8 Hz, $^4J_{H,H}$ = 1.7 Hz, $J_{C,H}$ = 162.4 Hz), 2.31(s, 3H, [3-OCOC*H*$_3$], $J_{C,H}$ = 131.5 Hz), 2.16(s, 3H, [7-OCOC*H*$_3$], $J_{C,H}$ = 129.6 Hz), 1.97(d, 3H, [3′-C*H*$_3$], $^3J_{H,H}$ = 7.0 Hz, $^4J_{H,H}$ = 1.7 Hz, $J_{C,H}$ = 130.2

Table 1. NMR Data for **1** and **3**−**5** in Acetone-d_6 at 400 MHz

	1 (1d)		**3 (3-ac)**		**4 (3,7-diac)**		**5 (3-ac,7-OMe)**	
pos	δ_C[a]	δ_H (mult., *J* = Hz)	δ_C[a]	δ_H (mult., *J* = Hz)	δ_C	δ_H (mult., *J* = Hz)	δ_C	δ_H (mult., *J* = Hz)
2	146.2		155.3		155.6		155.3	
1′	119.7	6.60 (m)	118.5	6.53 (dd,15.8, 1.5)	118.4	6.54 (dd,15.8, 1.7)	118.6	6.56 (dd,15.8, 1.7)
2′	132.9	6.60 (m)	138.3	6.79 (dd,15.8, 7.0)	138.8	6.80 (dd,15.8, 7.0)	138.3	6.80 (dd,15.8,7.0)
3′	18.9	1.97 (d[b])	19.0	1.96 (dt,7.0, 1.5)	19.0	1.97 (dt,7.0, 1.7)	19.0	1.97 (dt,7.0, 1.7)
3	n.d.[c]		n.d		137.9		137.9	
4	n.d.		n.d		167.6		167.6	
4a	n.d.		114.9		115.9		116.7	
5	165.3		164.9		165.3		165.2	
6		7.66 (vbr s)		7.73 (vbr s)		8.04 (br d)		7.88 (br s)
7	76.4	5.92 (s)	76.1	5.96 (s)	75.9	6.86 (d, 0.8)	82.5	5.88 (d, 0.8)
7a	175.2		176.4		173.5	-	174.3	
3-OH		n.d.						
7-OH		n.d.		n.d.				
3-OAc			168.4		168.2		168.1	
3-OAc			20.4	2.30 (s)	20.3	2.31 (s)	20.3	2.33 (s)
7-OAc					170.7			
7-OAc					20.8	2.16 (s)		
7-OMe							54.3	3.43 (s)

[a]Due to limited solubility, carbon resonances were detected indirectly via HSQC or HMBC. [b]Apparent doublet with extra peak inside. [c] n.d. = not detected.

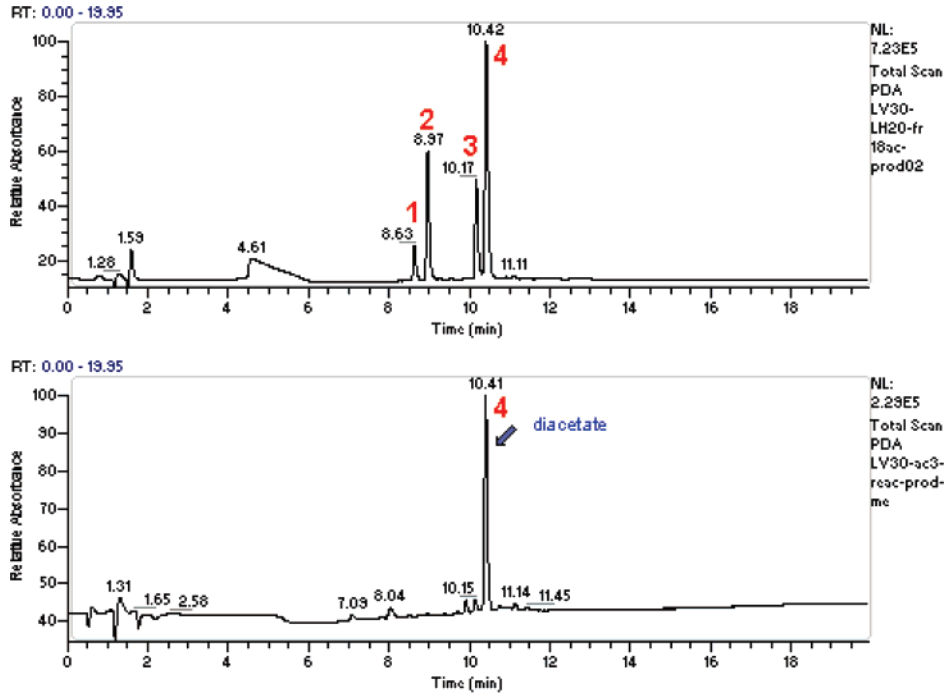

Figure 11. Acetylation products of pyranonigrin A (peak 1), 3-*O*-acetylpyranonigrin A (peak 2), 7-*O*-acetylpyranonigrin A (peak 3), and 3,7-di-*O*-acetylpyranonigrin A (peak 4).

Hz); MS (ESI-pos) $[M + H]^+ = m/z$ 308.0 (60%), $[M + NH_4]^+ = m/z$ 324.9 (15%), $[2M + H]^+ = m/z$ 614.9 (20%), $[2M + NH_4]^+ = m/z$ 631.8 (100%), $[3M + NH_4]^+ = m/z$ 938.2 (25%); MS(ESI-neg) $[2M - CH_3OOH]^- = m/z$ 553.6 (1.2%), $[2M + HCOO]^- = m/z$ 659.0 (2.8%)

5 (3-*O*-Acetyl-7-*O*-methylpyranonigrin A), 7-methoxy-4,5-dioxo-2-[(1*E*)-prop-1-enyl)]-4,5,6,7-tetrahydropyrano[2,3-*c*]pyrrol-3-yl acetate: $C_{13}H_{13}NO_6$ MW 279.25 (see Figure 5); $[\alpha]_D^{25}$ −2.7 ± 1 (*c* 0.75%, MeOH); UV (MeCN/H_2O) λ_{max} nm 216, 250 (sh), 286; ^{1}H NMR ($CDCl_3$) δ_H 8.06(br s, 1H, N*H*), 6.76(m, 1H, [H-2′], $^3J_{trans}$ = 15.8 Hz, $^3J_{H,H}$ = 7.0 Hz), 6.29(dd, 1H, [H-1′], $^3J_{trans}$ = 15.8 Hz, $^3J_{H,H}$ = 1.5 Hz), 5.70 (d, 1H, [H-7], $^3J_{H,H}$ = 1.5 Hz), 3.38 (s, 3H, OCH_3), 2.33(s, 3H, OCOCH_3), 1.96(d, 3H, [3′-CH_3], $^3J_{H,H}$ = 7.0 Hz, $^4J_{H,H}$ = 1.5 Hz); ^{13}C NMR ($CDCl_3$) δ_C 172.7(s, C-7a), 167.4(2s, C-4, O*C*OCH$_3$), 166.1 (s, C-5), 155.2(s, C-2), 138.5(d, C-2′), 136.7(s, C-3), 117.1(d, C-1′), 115.2(s, C-4a), 81.7(d, C-7), 54.3(q, O*C*H$_3$), 20.1(q, 3-OCO*C*H$_3$), 19.0-(q,C-3′); ^{1}H NMR (acetone-d_6) (see Table 1); ^{13}C NMR (acetone-d_6) (see Table 1); ^{1}H NMR (acetone-d_6) δ_H 6.80(m, 1H, [H-2′], $^3J_{trans}$ = 15.8 Hz, $^3J_{H,H}$ = 7.0 Hz, $J_{C,H}$ = 166.0 Hz), 6.56(dd, 1H, [H-1′], $^3J_{trans}$ = 15.8 Hz, $^4J_{H,H}$ = 1.7 Hz, $J_{C,H}$ = 162.4 Hz), 5.88 (d, 1H, [H-7], $^3J_{H,H}$ = 1.5 Hz), 3.43 (s, 3H, [OCH_3], $J_{C,H}$ = 143.1 Hz), 2.31(s, 3H, [OCOCH_3], $J_{C,H}$ = 130.9 Hz), 1.97(d, 3H, [3′-CH_3], $^3J_{H,H}$ = 7.0 Hz, $^4J_{H,H}$ = 1.7 Hz, $J_{C,H}$ = 130.2 Hz); MS (ESI-pos) $[M + H]^+ = m/z$ 280.1 (60%), $[2M + H]^+ = m/z$ 559.2 (20%), $[2M + NH_4]^+ = m/z$ 576.2 (100%); MS (ESI-neg) $[M - H]^- = m/z$ 278.0 (10%), $[2M + HCOO]^- = m/z$ 603.1 (100%).

6 (3-*O*-Ethylpyranonigrin A), 3-ethoxy-7-hydroxy-2-[(1*E*)-prop-1-enyl)]-6,7-dihydropyrano[2,3-*c*]pyrrole-4,5-dione): $C_{12}H_{13}NO_5$ MW 251.24. To a solution of **1** (10.0 mg) and iodoethane (50 μL) in dry DMF (200 μL) was added anhydrous Na_2CO_3 (20.0 mg). The mixture was stirred at ambient temperature for 16 h under argon. The solid was then removed by filtration, and the filtrate was evaporated to dryness under reduced pressure. The residue was then purified by HPLC on a C18 column (ODS-A, 30 × 250 mm, 5 μm) using a gradient of MeCN in H_2O both containing 0.01% TFA to obtain **6** as a white powder (5.2 mg): UV λ_{max} (nm) 216, 254, 298; ^{1}H NMR (DMSO-d_6) δ_H 8.59(d,$^3J_{H,H}$ = 0.8 Hz, 1H, N*H*), 6.78(d, 1H, [7-O*H*], $^3J_{H,H}$ = 8.8 Hz), 6.61(m, 1H, [H-1′], AB system), 6.60(m, 1H, [H-2′]), 5.72(dd, 1H, [H-7], $^3J_{H,H}$ = 8.8, 0.8 Hz), 4.04(q, 2H, [3-OCH_2−], $^3J_{H,H}$ = 7.0 Hz, $J_{C,H}$ = 146.0 Hz), $^3J_{H,H}$ = 7.0 Hz, $^4J_{H,H}$ = 1.7 Hz, $J_{C,H}$ = 130.2 Hz,), 1.24(t, 3H, [3-OCH$_2$CH_3], $^3J_{H,H}$ = 7.0 Hz, $J_{C,H}$ = 124.0 Hz), 1.97 (d, 3H, [3′-CH_3], $^3J_{H,H}$ = 7.0 Hz); ^{13}C NMR (DMSO-d_6) δ_C 174.7(s, C-7a), 170.0(s, C-4), 164.6(s, C-5), 154.3(s, C-2), 142.3(s, C-3), 134.9 (d, C-2′), 118.4(d, C-1′), 113.7(s, C-4a), 74.8(d, C-7), 67.9(t, 3-OCH_2−), 18.5(q,C-3′), 15.1(q, 3-OCH$_2$*C*H$_3$); MS (ESI-pos) $[M + H]^+ = m/z$ 252 (100%).

Acknowledgment. Our gratitude is extended to Prof. K. Nakanishi for his unfailing willingness to discuss all aspects of this work. Further, we appreciate the determination of molecular weights (HRMS) by our colleague X. Feng and the recording of ^{1}H−^{15}N HMBC data by R. T. Williamson. We also thank J. Ashcroft for his NMR instrument expertise at a time of critical need, as well as other co-workers in DAC and the Natural Products Section at Wyeth Research for their support in this project.

Supporting Information Available: ^{1}H NMR spectrum, ^{1}H−^{15}N HMBC spectrum, ^{1}H−^{13}C HMBC spectrum,^{1}H−^{13}C HSQC spectrum, ^{13}C NMR spectrum, UV spectra. This material is available free of charge via the Internet at http://pubs.acs.org.

References and Notes

(1) Ikeda, S.; Sugita, M.; Yoshimura, A.; Sumizawa, T.; Douzono, H.; Nagata, Y.; Akiyama, S. *Int. J. Cancer* **1990**, *45*, 508−513.
(2) Galmarini, O. L.; Mastronardi, I. O.; Priestap, H. A. *Experientia* **1974**, *30*, 586.
(3) Tanaka, H.; Wang, P.-L.; Yamada, O.; Tamura, T. *Agric. Biol. Chem.* **1966**, *30*, 107−113.
(4) Ehrlich, K. C.; DeLucca, A. J.; Ciegler, A. *Appl. Environ. Microbiol.* **1984**, *48*, 1−4.
(5) Bouras, N.; Mathieu, F.; Coppel, Y.; Lebrihi, A. *Nat. Prod. Res.* **2005**, *19*, 653−659.
(6) Buchi, G.; Klaubert, D. H.; Shank, R. C.; Weinreb, S. M.; Wogan, G. N. *J. Org. Chem.* **1971**, *36*, 1143−1147.
(7) Cutler, H. G.; Crumley, F. G.; Cox, R. H.; Hernandez, O.; Cole, R. J.; Dorner, J. W. *J. Agric. Food Chem.* **1979**, *27*, 592−595.
(8) Caesar, F.; Jansson, K.; Mutschler, E. *Pharm. Acta Helv.* **1969**, *44*, 676−690.
(9) Koegl, F.; Becker, H.; Detzel, A.; de Voss, G. *Liebigs Ann. Chem.* **1928**, *465*, 211−242.
(10) Gerhardt, P.; Dorrell, W. W.; Baldwin, I. L. *J. Bacteriol.* **1946**, *52*, 555−564.
(11) Karaffa, L.; Kubicek, C. P. *Appl. Microbiol. Biotechnol.* **2003**, *61*, 189−196.
(12) Hiort, J.; Maksimenka, K.; Reichert, M.; Perovic-Ottstadt, S.; Lin, W. H.; Wray, V.; Steube, K.; Schaumann, K.; Weber, H.; Proksch, P.; Ebel, R.; Müller, W. E. G.; Bringmann, G. *J. Nat. Prod.* **2004**, *67*, 1532−1543.

(13) Carletti, I.; Banaigs, B.; Amade, P. *J. Nat. Prod.* **2000**, *63*, 981−983.
(14) Gastmans, J. P.; Gastmans, D. F.; Ferraz, M. H. M. *Ecletica Quim.* **1979**, *4*, 71−77.
(15) Sterk, H.; Kappe, T.; Ziegler, E. *Monatsh. Chem.* **1968**, *99*, 2223−2226.
(16) Singh, S. B.; Zink, D. L.; Heimbach, B.; Genilloud, O.; Teran, A.; Silverman, K. C.; Lingham, R. B.; Felock, P.; Hazuda, D. J. *Org. Lett.* **2002**, *4*, 1123−1126.
(17) Ueno, M.; Amemiya, M.; Iijima, M.; Osono, M.; Masuda, T.; Kinoshita, N.; Ikeda, T.; Iinuma, H.; Hamada, M.; Ishizuka, M.; Takeuchi, T. *J. Antibiot.* **1993**, *46*, 1020−1023.
(18) Takahashi, S.; Kakinuma, N.; Iwai, H.; Yanagisawa, T.; Nagai, K.; Suzuki, K.; Tokunaga, T.; Nakagawa, A. *J. Antibiot.* **2000**, *53*, 1252−1256.
(19) Mase, N.; Nishi, T.; Takamori, Y.; Yoda, H.; Takabe, K. *Tetrahedron: Asymmetry* **1999**, *10*, 4469−4471.
(20) Issa, F.; Fischer, J.; Turner, P.; Coster, M. J. *J. Org. Chem.* **2006**, *71*, 4703−4705.
(21) Cuiper, A. D.; Kellogg, R. M. *Chem. Commun.* **1998**, 655−656.
(22) Burgstahler, A. W. *J. Am. Chem. Soc.* **1951**, *73*, 3021−3023.
(23) Leuchs, H.; Heller, A.; Hoffmann, A. *Ber. Dtsch. Chem. Ges.* **1929**, *62B*, 871−881.
(24) Wang, Y.; Raabe, G.; Repges, C.; Fleischhauer, J. *Int. J. Quantum Chem.* **2003**, *93*, 265−270.
(25) Braun, M.; Hohmann, A.; Rahematpura, J.; Bühne, C.; Grimme, S. *Eur.−J. Chem.* **2004**, *10*, 4584−4593.
(26) Schühly, W.; Crockett, S. L.; Fabian, W. M. F. *Chirality* **2005**, *17*, 250−256.
(27) Stephens, P. J.; McCann, D. M.; Devlin, F. J.; Smith, A. B. *J. Nat. Prod.* **2006**, *69*, 1055−1064.
(28) Stephens, P. J.; Devlin, F. J.; Cheeseman, J. R.; Frisch, M. J. *J. Phys. Chem. A* **2001**, *105*, 5356−5371.
(29) Wilson, S. M.; Wiberg, K. B.; Cheeseman, J. R.; Frisch, M. J.; Caccaro, P. H. *J. Phys. Chem. A* **2005**, *109*, 11752−11764.
(30) Devlin, F. J.; Stephens, P. J.; Besse, P. *J. Org. Chem.* **2005**, *70*, 2980−2993.
(31) He, J.; Wang, F.; Polavarapu, P. L. *Chirality* **2005**, *17*, S1−S8.
(32) Giorgio, E.; Roje, M.; Tanaka, K.; Hamersak, Z.; Sunjic, V.; Nakanishi, K.; Rosini, C.; Berova, N. *J. Org. Chem.* **2005**, *70*, 6557−6563.
(33) Devlin, F. J.; Stephens, P. J.; Bortolini, O. *Tetrahedron: Asymmetry* **2005**, *16*, 2653−2663.
(34) Maloney, K. N.; Hao, W.; Xu, J.; Gibbons, J.; Hucul, J.; Roll, D.; Brady, S. F.; Schroeder, F. C.; Clardy, J. *Org. Lett.* **2006**, *8*, 4067−4070.
(35) Abraham, W.-R.; Meyer, H.; Abate, D. *Tetrahedron* **1995**, *51*, 4947−4952.
(36) Wagner, C.; Anke, H.; Sterner, O. *J. Nat. Prod.* **1998**, *61*, 501−502.
(37) Tsukamoto, S.; Hirota, H.; Imachi, M.; Fujimuro, M.; Onuki, H.; Ohta, T.; Yokosawa, H. *Bioorg. Med. Chem. Lett.* **2005**, *15*, 191−194.
(38) Wang, C.-Y.; Wang, B.-G.; Brauers, G.; Guan, H.-S.; Proksch, P.; Ebel, R. *J. Nat. Prod.* **2002**, *65*, 772−775.
(39) Oh, H.; Swenson, D. C.; Gloer, J. B.; Shearer, C. A. *Tetrahedron Lett.* **2001**, *42*, 975−977.
(40) Samson, R. A.; Houbraken, J. A. M. P.; Kuijpers, A. F. A.; Frank, J. M.; Frisvad, J. C. *Stud. Mycol.* **2004**, *50*, 45−61.

NP070175N